Compound Nuclear Shell Effects in 14-MeV (n,α) Reactions*

APARESH CHATTERJEE
Saha Institute of Nuclear Physics, Calcutta, India
(Received 9 December 1963)

Smoothed curves drawn with suitable selection of 14-MeV reaction cross-section data reveal distinct shell effects. The cross section dips down at the proton shell and subshell closure positions throughout the mass region. Within a shell, the odd-even nucleon effects tend to disappear and the cross section is seen to be a very slowly decreasing function of the mass number. Across the shells, in addition to abrupt discontinuities, there is a gradual decrease of the cross sections from smaller to larger shells. These effects can be compared with various recent statements of the statistical level density. In the present work, the simple Bloch-Rosenzweig model of the shell-dependent form of the level density has been used and developed to study the effects. Results of computation reproduce the observed shapes faithfully up to $Z<50$; with plausible estimates about the combinatorial degeneracy in a major shell, good agreement with the assumption of the validity of the compound nuclear reaction at high excitation is obtained.

I. INTRODUCTION

MEASUREMENTS of the total (n,α) reaction cross sections with 14.8-MeV neutrons in four tellurium isotopes showed[1] that in this region (residual nuclear charge $Z_R=50$) there is a sharp drop in the cross section $\sigma_{n,\alpha}$. At lower Z_R values, the cross section is higher; as Z_R is increased beyond 50, $\sigma_{n,\alpha}$ gradually rises and reaches a maximum at $Z_R\simeq65$ and then slowly decreases to reach another minimum at $Z_R\simeq81$. The residual nuclei near the proton magic numbers 50 and 82 seemed to have very low cross sections compared to those of elements sufficiently far away from magic numbers.

In view of this interesting result, it was thought worthwhile to make a thorough and systematic search and compilation of the available results of the (n,α) cross sections at $E_n\simeq14$-MeV neutron energy. Such a compilation up to June 1963, reveals[2] that the whole mass region $(6<A<238)$ is reasonably well covered with only a few regions where no measurements exist and that many isotopic and a few isomeric cross-section data are available. It is also found that while most of the data lack in precision, they are *reliable* because the cross section seems to be insensitive to small neutron energy variations around 14.5 MeV. By selecting the data of the most abundant target elements, it is possible to prove the existence of a few clearly discernible trends.

It was noticed, for example, that there are no appreciable odd-even fluctuations in the cross section for nuclei away from magic numbers. But more interesting was the evidence of distinct proton shell and subshell effects throughout the mass region. In this work, we shall try to understand these effects from the viewpoint of the statistical theory of nuclear reactions.

II. OBSERVED SHELL EFFECTS

If we select the most abundant isotopes of the target elements, and plot $\sigma_{n,\alpha}$ against the corresponding Z_R values, we find[3] that the resulting smoothed average curve shows pronounced minima at all the magic proton numbers of the residual nuclei. In between the regions of a major proton-shell closure, the cross section reveals a flat peak somewhere in the middle.

Within a major shell, it is noted that subminima due to proton subshell closure are also sometimes clearly visible. In Fig. 1, we have plotted the data of the most abundant target elements up to medium weight nuclei $(Z_R<50)$. We notice that the closure of $1s_{1/2}$ (He^6), $1d_{5/2}$ (Si^{29}), $2p_{3/2,1/2}$ (Ga-Ge-As region) and $1f_{5/2}$ (Rb^{87}) proton subshells are distinctly marked by local drops in the cross-section values in addition to the main minima due to the closure of $1p_{1/2}$, $1d_{3/2}$, $1f_{7/2}$, and $1g_{9/2}$ shells at $Z_R=8$, 20, 28, and 50 (marked as curves a, b, c, and d).

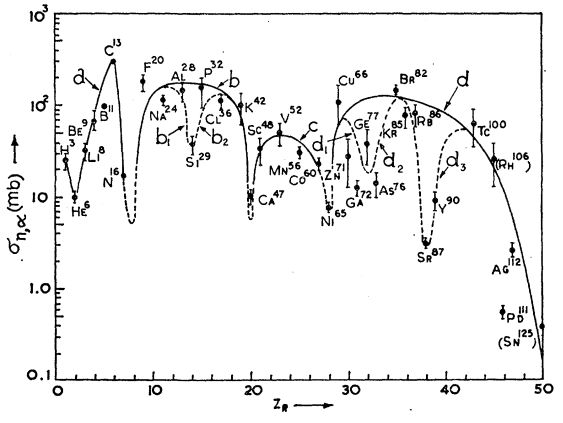

FIG. 1. Cross sections in mb for (n,α) reactions with 14-MeV neutrons against residual nuclear charge Z_R between 0 and 50. Reactions with most abundant target nuclei only are shown (except those marked as Ca^{47}, Ni^{65}, Rh^{106}, and Sn^{125} residual nuclei). For several existing measurements of one element, the average value has been used with appropriate estimated errors. The major proton shell regions are marked as a, b, c, and d.

* Paper contributed to the American Physical Society topical conference on Compound Nuclear States held in Gatlinberg, Tennessee, Oct. 10–12, 1963; the present text has been slightly modified.

[1] N. K. Majumdar and A. Chatterjee, Nucl. Phys. **41**, 192 (1963); A. Chatterjee, in Proceedings of a Symposium on Nuclear Physics, Bombay, 1963, p. 166 (unpublished).

[2] A. Chatterjee, Nucleonics (to be published).

[3] A. Chatterjee, Nucl. Phys. **47**, 511 (1963); Nucl. Phys. **49**, 686 (1963).

The information on heavy nuclei ($Z_R>50$) is summarized in Fig. 2. The minima due to $1g_{9/2}$ and $1h_{11/2}$ proton shell closure are clearly seen. Subminima due to the closure of $2d_{3/2}$ and $1g_{7/2}$ proton shells (marking, respectively, approximately the beginning and the end of the occurrence of rare-earth residual nuclei) are rather indistinctly seen as two valleys marked B and C.

III. COMPOUND NUCLEAR REACTION CROSS SECTION AND LEVEL DENSITY

We assume that the (a,ν) reaction initiated by the particle a with channel energy E_a proceeds only through the formation of a compound nucleus. Since we are interested in its properties averaged over an energy interval much larger than level widths or spacings, the statistical-model description will be adequate. Application of the principle of detailed balance will lead to the Weisskopf-Ewing formula relating the cross section $\sigma_{a,E\nu}$ to the level density ρ_ν of the *residual* nucleus (after Ericson[4] and Gove and Nakasima[5]) as

$$\sigma_{a,E\nu}=\sigma_c(a)\frac{g_\nu\mu_\nu\sigma_\nu^*(E_\nu)\rho_\nu(E_\nu^*)}{\sum_i g_i\mu_i\int_0^\infty E_i\sigma_i^*(E_i)\rho_i(E_i^*)dE_i}, \quad (1)$$

where $\sigma_c(a)$ is the cross section of formation of the compound nucleus C; g_i and μ_i are the intrinsic spin states ($\equiv 2s_i+1$) and reduced mass for the open channels i including ν (photon emission neglected) for the residual nucleus; $\sigma_i^*(E_i)$ is the "inverse" cross section at excitation E_i and $\rho_i(E_i^*)$ is the level density at excitation U_i-E_i for the exit channel i. We assume that the inverse cross section of a highly excited residual nucleus is the same as that in its ground state.

The evaporation approximation of the compound nucleus C ensures purely classical trajectories of the particles i in absence of the Coulomb barrier B_i and for a constant nuclear temperature T for the system. Therefore

$$\sigma_i^*(E_i)\simeq\sigma_i(E_i)=\pi R^2(1-k_iB_i/E_i), \quad (1a)$$

and

$$\rho_i(E_i^*)=\rho_i(U_i-E_i)=\rho_i(U_i)\exp(-E_i/T). \quad (1b)$$

Here R is the nuclear radius, k_iB_i is the "effective" Coulomb barrier for a height B_i and U_i is the highest energy available to the residual nucleus after emission of i as determined by the reaction energy (Q value) of the (a,i) reaction

$$U_i=E_a+Q_{a,i} \quad (1c)$$

by ignoring pairing and other corrections to U_i.

From (1) and (1b), the energy spectrum of the emitted particles is such that $\sigma_{a,Ei}$ is proportional to

$$(E_i-B_i)\exp(-E_i/T) \quad \text{for} \quad E_i>B_i.$$

Integration over E_i by assuming T and R to be constant for all decay channels and for all neighbors, respectively, gives the cross section of the (a,ν) reaction as

$$\sigma_{a,\nu}=\sigma_c(a)\frac{g_\nu\mu_\nu\rho_\nu(U_\nu-k_\nu B_\nu)}{\sum_i g_i\mu_i\rho_i(U_i-k_iB_i)}. \quad (2)$$

We further assume that the effect of the barrier of height B_i is negligible for particle emission in the compound nucleus with $U_i>B_i$. This is permissible because the level density appears in the form of a ratio in (2) and the integration from 0 to ∞ over E_i is essentially an integration involving an energy range a few times T near B_ν (say $B_\nu-T$ to $B_\nu+2T$). We therefore denote $\rho_i(U_i-B_i)$ as $\rho_i(U_i,j_i)$. The phase-space description in (1) now does not contain the implicit assumption of randomization over angular momenta. We shall make use of the removal of this restriction over the channel angular momentum j_i.

In case of (n,α) reactions leading to high excitation of the residual nucleus, the reaction cross section can be written as

$$\sigma_{n,\alpha}=\sigma_c(n)\frac{g_\alpha\mu_\alpha\rho_\alpha(U,j)}{\sum_i g_i\mu_i\rho_i(U,j)}, \quad (2a)$$

where $\sigma_c(n)$ is the neutron absorption cross section; the denominator contains contribution due to the competing processes like $(n,2n)$, (n,p), etc. In what follows, we shall omit the subscript on the level density. Our information of the compound nuclear reaction will depend very much on our knowledge of $\rho(U,j)$.

The level density $\rho(U,j)$ is usually expressed in the

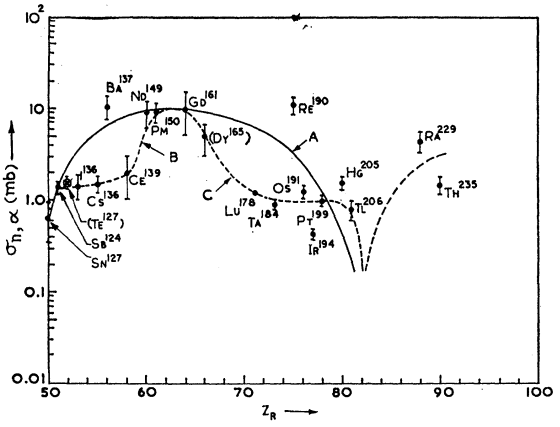

FIG. 2. Cross sections in mb for 14-MeV (n,α) reactions against Z_R between 50 and 100. Except for Te^{127} and Dy^{165}, reactions with most abundant target nuclei only are shown. The average of several measurements for an element, when existing, are shown; errors shown are estimates (usually the largest quoted). The regions B and C mark approximately the beginning and end of the occurrence of the rare-earth nuclei. The major shell is marked A.

[4] T. Ericson, Advan. Phys. **9**, 425 (1960).
[5] N. B. Gove and R. Nakasima, Nuovo Cimento **22**, 158 (1961).

free-gas model of two Fermions in the form[4]

$$\rho(U,j)=\frac{\pi}{3}(2j+1)\exp\left[-\frac{\hbar^2 j(j+1)}{2\tau t}\right]\frac{\hbar^3}{32\sqrt{2}\tau^{3/2}} \times\left(\frac{A}{\epsilon}\right)^{1/2}\cdot\frac{1}{U^2}\exp\pi\left(\frac{AU}{\epsilon}\right)^{1/2}. \quad (3)$$

Here A is the mass number, U is the excitation energy, ϵ is the Fermi energy, and the single-particle level density g_0 is defined in terms of equidistant individual Fermion-level spacings d_n and d_p as

$$g_0=\frac{1}{d_n}+\frac{1}{d_p}\equiv\frac{2}{d}=g_n+g_p\equiv 2g=\frac{3A}{2\epsilon}. \quad (4)$$

The spin-dependent part in (3) is

$$\rho_j(U,A)\equiv\rho_j-\rho_{j+1}=(2j+1)\exp[-\hbar^2 j(j+1)/2\tau t]. \quad (5)$$

The rigid-body moment of inertia τ in (3) and (5) is easily shown to be

$$\tau=\left(\frac{3}{\pi}\right)^{2/3}\frac{9}{10}\frac{A^{5/2}}{2\epsilon}\hbar^2. \quad (6)$$

The thermodynamic temperature t and the nuclear temperature T are related to g_0 and U by

$$\frac{1}{T}=\frac{1}{t}-\frac{2}{U}\simeq(\pi^2 g_0/6U)^{1/2}. \quad (7)$$

For high excitations, t can be replaced by T.

The U-dependent part of (1) can be expressed as

$$\rho(U,A)=U^{-2}\exp\pi(AU/\epsilon)^{1/2} \quad (8)$$

neglecting the small U dependence of $\rho_j(U,A)$ in (5).

It is easy to show that making use of (4) to (7), the total level density in (3) can be written in the form

$$\rho(U,j)=K[(2j+1)/A^2]P_j(U,A), \quad (9)$$

where

$$K=(\pi^2 5^{3/2}\epsilon/3^5 2^{5/2}), \quad (10)$$

and

$$P_j(U,A)=\rho(U,A)\times\exp[\tfrac{1}{2}\pi j(j+1)A^{-5/3}(AU/\epsilon)^{1/2}]. \quad (11)$$

We now consider approximately the effect on $\rho(U,j)$ of a shift in excitation energy from U to U'. If the shifted excitation energy U' is known to be related to U by a functional relationship of the form

$$U'=U+f \quad (f<U), \quad (12)$$

where f contains all the information causing such a shift, we have, to the first order,

$$(U')^n=U^n(1+nf/U). \quad (13)$$

Therefore $P_j(U',A)$ in (11) is obtained in the free-gas model as

$$P_j(U',A)=P_j(U,A)\frac{\exp[\tfrac{1}{2}\pi(A/\epsilon U)^{1/2}f]}{1+2f/U} \quad (14)$$

by restricting[6] the U variation only to (8).

IV. SHELL-DEPENDENT FORM OF THE LEVEL DENSITY

We now assume that the shell effects in the level density $\rho(U,j)$ are describable in terms of a suitable shift function in (12). For simplicity, we choose the Bloch-Rosenzweig model[7]. We ignore pairing and other correlation corrections and assume that the excitation energy U is not seriously altered by these corrections.

In our notation, Rosenzweig's description of the shell effects is expressed in terms of the shift function f as

$$f=\tfrac{1}{12}N^2 d_n+\tfrac{1}{12}P^2 d_p-\tfrac{1}{2}d_n(n-\tfrac{1}{2}N)^2-\tfrac{1}{2}d_p(p-\tfrac{1}{2}P)^2. \quad (15)$$

We recall that d_n and d_p appear in (4). The nucleons have variable occupation numbers n and p in a neutron and a proton subshell with highest allowable occupation numbers N and P, respectively.

$$0\leqslant n\leqslant N, \quad 0\leqslant p\leqslant P. \quad (16)$$

The highest occupation numbers N and P are really the total nucleon spin degeneracies of the different shell-model j states.

$$N\equiv(2j_N+1), \quad P\equiv(2j_P+1). \quad (17)$$

In (15), n (or p) particles occupying a subshell N (or P) have identical rearrangement probabilities as those of $N-n$ (or $P-p$) holes in that particular subshell. The relationship (15) is an approximation, breaks down for N (or P) >12 ($>1h_{11/2}$ subshells), and is suitable to use for high excitations ($U>f$).

Using (9), (11), (14), and (15), we can now write down the shell-dependent form of the total level density $\rho(U_s,j)\equiv\rho(U',j)$. After some algebra, on rearranging the terms, this is found to be

$$\rho(U_s,j)=\rho_0\frac{\exp[-(\pi/36)(\epsilon/AU)^{1/2}(N^2+P^2)(1+x)]}{1-[\epsilon(N^2+P^2)/9AU](1+x)}, \quad (18)$$

where

$$\rho_0=K(1/A^2)2(j_N+j_P+1)\,.\;P_j(U,A) \quad (19)$$

$$x=12\frac{n^2+p^2-nN-pP}{N^2+P^2} \quad (20)$$

[6] The exact $P_j(U',A)=\lambda\exp[\tfrac{1}{4}\pi j(j+1)A^{-5/3}(A\epsilon/U)^{1/3}f]$, where λ is the right-hand side of (14); this exponential coming through $\rho_j(U,A)$ in (5) has been neglected in (14).

[7] C. Bloch, Phys. Rev. **93**, 1094 (1954); N. Rosenzweig, Phys. Rev. **105**, 950 (1957); **108**, 817 (1957); N. Rosenzweig, L. M. Bollinger, L. L. Lee, and J. P. Schiffer, *Proceedings of the Second International Conference on the Peaceful Uses of Atomic Energy, Geneva, 1958* (United Nations, Geneva, 1958), paper 693, p. 11.

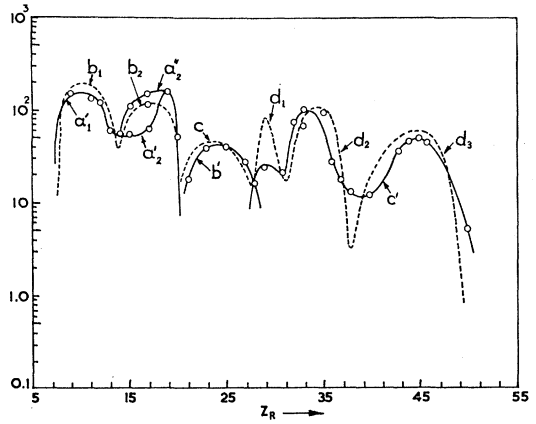

FIG. 3. The computed curves (full lines) against $Z_R(9 \leqslant Z_R \leqslant 55)$ obtained from the analysis of the present work. The regions of the three major proton shells a, b, c use different normalizing factors ρ_0 (see text). The ordinate is $\rho(U_s,j)/\rho_0$; for features a_2' and a_2'', see text. The dotted curves b, c, and d are the same as in Fig. 1; it has been superimposed here for comparison.

$$=0 \text{ for a completely full or empty shell } (N,P) \quad (21)$$

$$=-3 \text{ for a half-filled shell } (N/2,\ P/2). \quad (22)$$

Equation (18) is in a suitable form for numerical computation. For the actual residual nuclei of Figs. 1 and 2, we can now compute the values of $\rho(U_s,j)$ by noting the appropriate values of n, N, p and P. For observing the gross trends, it is adequate to treat ρ_0 as a normalizing factor whose value remains constant within a shell ("fixed A" assumption) but varies from shell to shell.

A more general and appropriate description for ρ_0 would be to replace (19) by

$$\rho_0 = K(1/A^2)P_j(U,A)(\sum N + \sum P) \quad (19a)$$

when the subshell states are mixed in a major shell, implying a higher combinatorial degeneracy than expressed in (5).

We note that for 14-MeV neutrons, the Q value is $Q_{n,\alpha} \simeq +5$ MeV for medium weight and heavy nuclei. The excitation energy U is therefore $\simeq 20$ MeV, and it is permissible to set $U/\epsilon \simeq 1$. This assumption, somewhat unjustified for the light nuclei, has been used throughout this work.

V. FIT WITH THE OBSERVED DATA

The results of numerical computation of (18) have been shown in Fig. 3 as $\rho(U_s,j)/\rho_0$ against Z_R between 9 and 50 ($16 < A < 130$). The observed cross sections of Fig. 1 are also shown for comparison. Values of ρ_0 from shell to shell determines the real values of $\rho(U_s,j)$. For convenience the computed curves in different regions have been marked as a', b', c', etc. The lightest nuclei below N^{16} have not been considered.

In the $1f_{7/2}$ proton shell (curve b'), a very good fit is observed with the experimental curve c with the peak fitted with a normalizing factor of 12. The shape, the sharp rise and fall in the regions of shell closure, and the flat peak in the midshell region are faithfully reproduced in curve b'. Only a negligible mixing with the various neutron subshell states occur here. Therefore the total j degeneracy ($\simeq 16$) times $1/A^2$ brings this close to the actually used normalizing factor.

In the preceding major shell (curve a'), the fit in the region of $1d_{5/2}$ proton shell is again very good with a normalizing factor of 40. The $d_{5/2}$ shell closure at Si^{29} is clearly seen. In the heavier region, the $s_{1/2}$, $d_{3/2}$ subshells are not well separated. Therefore, two curves a_2' and a_2'' have been shown corresponding to the separated and unseparated degeneracies, respectively. Both these curves predict a second subpeak near K^{42} residual nucleus, which is actually observed; the smoothed experimental curve b_2 passes in between a_2' and a_2''. The total major shell degeneracy times $1/A^2 = 40$ (we have arbitrarily set $1/A^2$ around $A = 15$ as unity throughout).

In the third region marked c', subshell closure occurs near the Ga-Ge-As nuclei and at Sr^{87}. A normalizing factor of 16 has been used for this region. Disregarding the only existing data[8] on Cu^{66}, the fit is not bad, giving the subdip at Ga^{72} and the peak at Br^{82}. The very large drop coinciding with the closure of the $1g_{9/2}$ proton shell is also clearly seen.

VI. DISCUSSION

The depths of the main double shell-closure dips are accurately described by Eq. (18) with $x=0$, provided the occupation number n for neutrons is also zero. This will provide the "background" on which the contribution due to shell, pairing, and other effects will be superimposed. However, such "ideal" nuclei do not exist in nature. In the present work, computations were made on the actual residual nuclei.

The parity mixing effects have been ignored. It has been shown[4] that a 20% mixing of parity of one kind with 80% of the other changes the equal probability of both parities by only $\pm 4\%$.

It is generally assumed[4] that the shell effect predicted by the Rosenzweig form is small and is insufficient to use except near the closure of the $1g_{9/2}$ shells. The present analysis, involving about 200 experimental data, uses this simple form and shows that it is adequate to describe compound nuclear-shell effects even at high excitations ($U/\epsilon \simeq 1$).

The above analysis of the shell effects can be extended to and combined with the Lang and LeCouteur form[9] of the level density. This pairing model was not considered for 14-MeV (n,α) reactions since the average pairing corrections would be $\sim 5\%$ in U. For lower excitations, the shell-dependent pairing model should be used, e.g., for isotopic-reaction cross sections.

[8] E. B. Paul and R. L. Clarke, Can J. Phys. **31**, 267 (1963).
[9] J. M. Lang and K. J. Le Couteur, Nucl. Phys. **14**, 21 (1959).